Earthquakes and Structures, *Vol. 18, No. 1 (2020) 27-44*
DOI: https://doi.org/10.12989/eas.2020.18.1.027

A comparison of three performance-based seismic design methods for plane steel braced frames

Nicos A. Kalapodis[1a], George A. Papagiannopoulos[*2] and Dimitri E. Beskos[3,4b]

[1]*Department of Engineering Science, University of Greenwich, Central Avenue, ME4 4TB Chatham, U.K.*
[2]*School of Science and Technology, Hellenic Open University, 26335 Patras, Greece*
[3]*Department of Disaster Mitigation for Structures, College of Civil Engineering, Tongji University, Shanghai 200092, PR China*
[4]*Department of Civil Engineering, University of Patras, 26054 Patras, Greece*

(*Received August 1, 2019, Revised October 31, 2019, Accepted September 13, 2019*)

Abstract. This work presents a comparison of three performance-based seismic design methods (PBSD) as applied to plane steel frames having eccentric braces (EBFs) and buckling restrained braces (BRBFs). The first method uses equivalent modal damping ratios (ξ_k), referring to an equivalent multi-degree-of-freedom (MDOF) linear system, which retains the mass, the elastic stiffness and responds in the same way as the original non-linear MDOF system. The second method employs modal strength reduction factors ($\bar{q}_k$) resulting from the corresponding modal damping ratios. Contrary to the behavior factors of code based design methods, both ξ_k and $\bar{q}_k$ account for the first few modes of significance and incorporate target deformation metrics like inter-storey drift ratio (IDR) and local ductility as well as structural characteristics like structural natural period, and soil types. Explicit empirical expressions of ξ_k and $\bar{q}_k$, recently presented by the present authors elsewhere, are also provided here for reasons of completeness and easy reference. The third method, developed here by the authors, is based on a hybrid force/displacement (HFD) seismic design scheme, since it combines the force-base design (FBD) method with the displacement-based design (DBD) method. According to this method, seismic design is accomplished by using a behavior factor (q_h), empirically expressed in terms of the global ductility of the frame, which takes into account both non-structural and structural deformation metrics. These expressions for q_h are obtained through extensive parametric studies involving non-linear dynamic analysis (NLDA) of 98 frames, subjected to 100 far-fault ground motions that correspond to four soil types of Eurocode 8. Furthermore, these factors can be used in conjunction with an elastic acceleration design spectrum for seismic design purposes. Finally, a comparison among the above three seismic design methods and the Eurocode 8 method is conducted with the aid of non-linear dynamic analyses via representative numerical examples, involving plane steel EBFs and BRBFs.

Keywords: modal strength reduction factors; equivalent modal damping ratios; HFD seismic design; steel braced frames

1. Introduction

Provided a realistic modeling of a structure is possible, the most accurate way to compute its seismic response is by conducting a non-linear (including both material and geometrical non-linearities) dynamic analysis (NLDA) in conjunction with the finite element method (FEM) in the time domain. Despite its validity, the non-linear dynamic analysis method constitutes a rather inconvenient way of seismic design, since it requires an advanced modeling of the real structure and a large number of ground motions. To overcome these difficulties, the last 50 years or so researchers have developed more simplified procedures for seismic design of structures. Since engineers are more familiar with forces as design parameters, all modern seismic design codes like Eurocode 8 (2009) have adopted the force-based seismic design method (FBD) in conjunction with the acceptance that structures respond inelastically and absorb seismic energy. Damages are permitted up to a certain extent but collapse must be avoided. The main tool that modern codes use for applying linear analysis is the acceleration response spectrum. The inelastic behavior is considered by dividing the elastic acceleration response spectrum ordinates by the strength reduction factor *(q)*, which is indicative of the global ductility and over-strength of the structure (Eurocode 8 2009).

A more recent seismic design method is the displacement-based design (DBD) method, where displacements are the main design parameters. Since displacements are closely related to damage, by controlling them one can control the damage level of the structure, from the beginning of the design procedure (Priestley *et al.* 2007, Salawdeh and Goggins 2016). The most widespread method in the field of DBD, is the direct displacement-based design (DDBD), where the non-linear multi-degree-of-freedom (MDOF) system is reduced to an equivalent linear single-degree-of-freedom (SDOF) system and the maximum base shear force is evaluated by means of a displacement design spectrum (Priestley *et al.* 2007).

Performance-based seismic design of structures (PBSD) constitutes the most current trend that takes the probability

∗Corresponding author, Instructor
E-mail: papagiannopoulos.georgios@ac.eap.gr
[a]Post Doctoral Research Associate
[b]Emeritus Professor

http://www.techno-press.org/?journal=eas&subpage=7 ISSN: 2092-7614 (Print), 2092-7622 (Online)

of occurrence of a seismic excitation into consideration and drives to a more realistic seismic design (SEAOC 1999, Li *et al.* 2017). According to PBSD, the structure is designed for various performance levels, with each one of them defined by a pair of damage level (in terms of IDR and/or local ductility) and seismic intensity (in terms of return period of the earthquake). Despite the fact that Eurocode 8 (2009) endorses the concept of PBSD, it makes limited use of it. More specifically, seismic design according to Eurocode 8 (2009) accounts for two performance levels. First, seismic design for the performance level of life safety (LS) is conducted by means of strength satisfaction under the design basis earthquake. Then, the design continues with the damage limitation (DL) performance level by checking the deformation limitation of the structure under the frequently occurred earthquake. Thus, there is a need for the development of rational yet practical seismic design methods, that will include strength and displacement control under a PBSD framework.

This paper presents a comparison among three performance-based seismic design methods, as well as the Eurocode 8 (2009) seismic design method as applied to steel plane frames having eccentric braces (EBFs) and buckling restrained braces (BRBFs) with the aid of non-linear dynamic analysis (NLDA) on the basis of representative numerical examples. The first two methods make use of modal damping ratios and modal strength reduction factors, based on the original works of Papagiannopoulos and Beskos (2010, 2011) on steel plane moment resisting frames (MRFs). These works were later very much improved by more refined modeling and inclusion of a substantially larger number of frames and ground motions by Loulelis *et al.* (2018) who considered MRFs and Kalapodis *et al.* (2018), Kalapodis and Papagiannopoulos (2020) who considered braced frames. More specifically, the first method is a FBD one, using equivalent modal damping ratios ξ_k (for the first k modes of significance) and an elastic response (design) spectrum modified for high amounts of damping in order to determine the design base shear force of the structure. These modal damping ratios ξ_k : i) are computed for an equivalent linear MDOF system which has the same mass and elastic stiffness with the corresponding original non-linear one and ii) are expressed as functions of the corresponding natural periods of the structure T_k, the target structural deformation in terms of IDR and/or local ductility of the dissipative members and the soil class according to the categorization of Eurocode 8 (2009). The second seismic design method is also a FBD method based upon the same conceptual framework as the first one and incorporates equivalent modal strength reduction (or behavior) factors q_k, which are obtained from the corresponding ξ_k and also correspond to the first k modes of significance. Use of these modal factors q_k in conjunction with the elastic design spectrum of Eurocode 8 (2009) leads to the design base shear of the structure. These two methods have also been very recently extended to the seismic design of plane reinforced concrete (R/C) frames with or without infills and walls by Muho *et al.* (2019a & b). A brief description of the above two seismic design methods together with explicit expressions for ξ_k and q_k on the basis of the works of Kalapodis *et al.* (2018) and Kalapodis and Papagiannopoulos (2020) are provided in this work for reasons of completeness and easy reference.

The third method is a hybrid force/displacement (HFD) seismic design method, which originally has been developed for steel plane and space MRFs by Karavasilis *et al.* (2006) and Tzimas *et al.* (2013). More recently, this method has been extended from steel to plane composite steel/concrete structures by Skalomenos *et al.* (2015) and to plane R/C structures by Pian *et al.* (2019) The main characteristic of this method is that combines the best elements of both FBD and DBD methods, while at the same time eliminates their disadvantages. HFD is a FBD method, since one can make use of the well-known acceleration design spectrum in conjunction with a deformation-dependent behavior (strength reduction) factor q_h, which is the same for all modes of the frame. Hence, the HFD method is compatible with all commercial software packages for seismic design of structures and preserves familiar to engineers concepts. The HFD seismic design method is extended in this paper to the case of steel plane EBFs and BRBFs. Explicit empirical expressions for the behavior or strength reduction factor q_h as function of period, deformation/damage and soil class are derived by regression analysis on the basis of a large response databank created by extensive NLDA involving 98 steel plane braced frames under 100 far-field seismic excitations.

The main advantages of the three seismic design methods considered herein over the code based FBD is that ξ_k, q_k and q_h take into account the dynamic structural characteristics, the difference in soil types and the variation of the performance targets, instead of using a behavior or strength reduction factor q which only depends on structural typology. Thus, contrary to code based FBD, there is no need for deformation checks since the three methods automatically satisfy these checks and for each selected performance level. Furthermore, in comparison with the DBD, the three methods considered here are more accurate since they replace the non-linear MDOF system by an equivalent linear MDOF instead of a SDOF system, retaining, thus, the significant structural dynamic characteristics. Contrary to the DBD, these three methods utilize the more familiar to engineer's acceleration design spectra instead of displacement design spectra. Analytical period-dependent expressions for ξ_k, q_k and q_h in connection with a deformation/damage level and soil type are provided in the form of tables. These expressions are derived through extensive parametric analyses of 98 steel plane braced frames under 100 far-field seismic motions. In the cases of the second and third methods mentioned previously, these expressions can be applied to a typical 5%-damped elastic design spectrum for the seismic design purposes of the steel braced frame. The first method requires an enhancement of the conventional elastic pseudo-acceleration spectra by adding curves for values of damping higher than 5%. The three methods considered here are illustrated by representative examples that also serve to compare them to each other and demonstrate their advantages over code based seismic design methods.

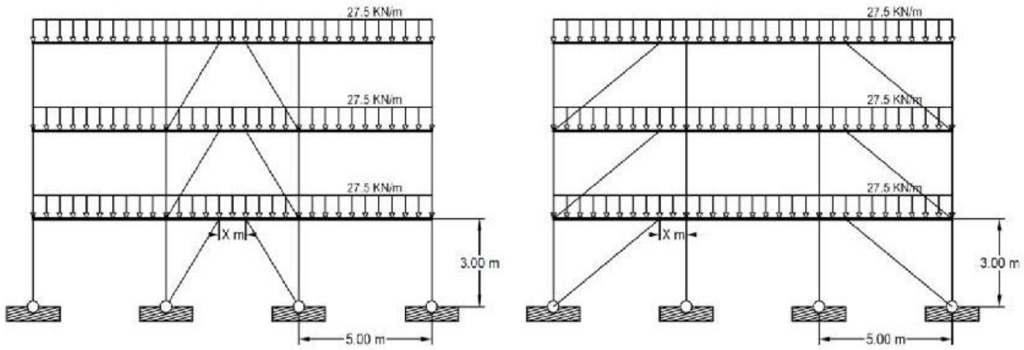

Fig. 1 Configuration of the EBFs considered: chevron bracing (left) and diagonal bracing (right)

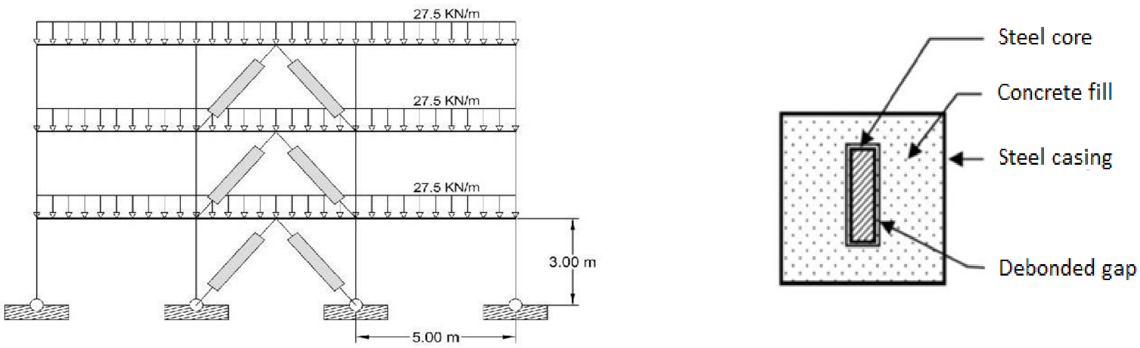

Fig. 2 Configuration of BRBFs considered (left) and cross section the BRB (right)

2. Seismic design methods based on ξ_k and q_k

This section briefly describes the first two considered here seismic design methods based on ξ_k (Papagiannopoulos and Beskos 2010) and q_k (Papagiannopoulos and Beskos 2011) as applied to steel plane EBFs and BRBFs for reasons of completeness and easy reference. Figs. 1 and 2 depict the geometrical characteristics of these two types of braced frames considered here. Table 1 provides a categorization of seismic links for the EBFs.

2.1 Method based on equivalent modal damping ratios (ξ_k)

This method is a FBD one, which determines the design base shear of a steel plane frame by using a pseudo-acceleration elastic design spectrum modified to include high amounts of viscous damping ratios ξ (5%<ξ<100%) in conjunction with ξ_k for the first few k significant modes of the structure in a modal superposition approach. These equivalent modal damping ratios ξ_k are defined from an equivalent linear MDOF system to the original nonlinear one so that the work of dissipation due to viscous forces in the former system balances that due to inelastic forces in the later one. Thus, equivalence is defined here only with respect to damping and not with respect to damping and stiffness or period as it is the case in most of the existing works on equivalent linearization, which are also restricted to single degree of freedom (SDOF) systems equivalent to MDOF ones. A recent discussion by Papagiannopoulos (2018) on the concept of equivalent damping is worth mentioning it.

Parametric seismic inelastic time-history analyses of the EBFs and BRBFs are conducted (Kalapodis *et al.* 2018) in order to compute the ξ_k values that correspond to four seismic performance levels (SP), i.e., immediate occupancy (IO), damage limitation (DL), life-safety (LS) and collapse prevention (CP). For the EBFs, the values of IDR, link ductility μ_θ and link rotation θ_{link} associated with the four SP levels are stated in Table 2, following SEAOC (1999) and Eurocode 8 (2009).

In absence of any SP level expressed by IDR and axial ductility μ_δ of the buckling-restrained braces (BRBs) in SEAOC (1999) and Eurocode 8 (2009), the IDR values of Table 2 have been also used for the BRBFs, whereas μ_δ values are approximated on the basis of those proposed by Bosco *et al.* (2015).

Tables 3-7 provide expressions for ξ_k for the first four modes and the aforementioned four SP levels, as functions of the period T for various types of steel plane EBFs and BRBFs. These tables are restricted to the case of soil class B. Additional tables covering the cases of soil class A, C and D can be found in Kalapodis (2017).

Table 1 types of seismic links of length X in EBFs of Fig. 1

Type of link	Equal moments at both ends	Non-equal moments at both ends*
Shear	$X < X_s = 1.6M_{p,l}/V_{p,l}$	$X < X_s = 0.8(1+\alpha)\ M_{p,l}/V_{p,l}$
Flexural	$X > X_F = 3.0M_{p,l}/V_{p,l}$	$X > X_F = 1.5(1+\alpha)M_{p,l}/V_{p,l}$
Intermediate	$X_s < X < X_F$	$X_s < X < X_F$

Table 2 Seismic performance (SP) levels

SP level	IDR	μ_θ	θ_{link} (rad)	μ_δ
SP1-IO	0.004	1.0	Not provided	1.0
SP2-DL	0.013	3.6	Not provided	3.5
SP3-LS	0.022	6.2	0.02 (flexural links) 0.08 (shear links)	6.3
SP4-CP	0.032	8.0	Not provided	Not provided

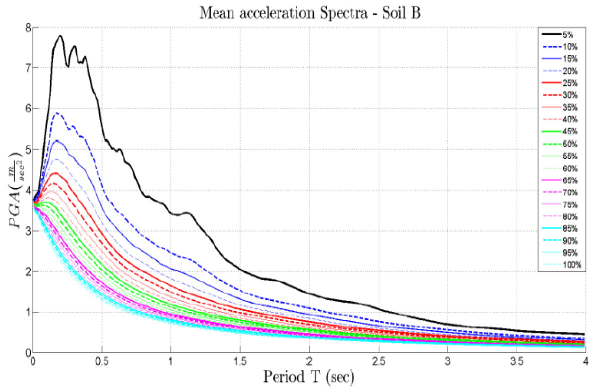

Fig. 3. Mean acceleration spectra derived for soil class B and several viscous damping ratios

Fig. 3 depicts mean values of pseudo-acceleration design spectra derived from 25 seismic motions compatible to the Eurocode 8 (2009) design spectrum for high viscous damping ratios ξ (5%<ξ<100%) and soil class B. The corresponding spectra for the cases of soil classes A,C and D can be found in Kalapodis (2017). At this point one should stress that acceleration response spectra for high values of ξ are absolute, meaning that the inertia force is equal to the elastic restoring force plus the damping force, which cannot be neglected for high ξ values. These absolute acceleration spectra are converted into pseudo ones, like those in Fig. 3, where inertia force is equal only to the elastic restoring force by following Hatzigeorgiou (2010). For more details on the construction of these spectra, one should consult Kalapodis (2017). Computation of displacement is not needed since these are automatically satisfied by using the ξ_k, which are deformation dependent. Thus, use of the approximate equal displacement rule for displacement determination, as performed in the context of Eurocode 8 (2009), is avoided.

It should be noted that values of ξ_k in excess of 100% have been computed for the collapse prevention (CP) seismic performance level. However, for the CP performance level, according to Papagiannopoulos and Beskos (2010), one has to use ξ_k=100% for all k modes. Thus, design equations of ξ_k for the CP performance level are omitted in Tables 3-7.

2.2 Method based on modal behavior factors (q_k)

This method is also a FBD method, which determines the design base shear of a steel plane frame by using a code based pseudo-acceleration elastic design spectrum in conjunction with modal behavior (strength reduction) factors q_k for the first few k significant modes of the structure in a modal superposition approach. These modal behavior factors q_k are calculated from the equivalent modal damping ratios ξ_k with the aid of the modal damping reduction factor $B_{d,k}$ defined as $B_{d,k} = S_{a,k}(T,\xi_k)/S_{a,k}(T,5\%)$ where $S_{a,k}(T,\xi_k)$ represents the absolute maximum acceleration for $\xi_k > 5\%$. Thus, one can easily prove that the absolute modal behavior factor q_k defined as the ratio of the modal elastic base shear $V_{el,k}$ over the modal base shear at first yielding $V_{y,k}$ is equal to $1/B_{d,k}$. The absolute q_k thus obtained, can be converted to $\bar{q}_k$, which is compatible with the pseudo-acceleration design spectrum of Eurocode 8 (2009) as explained in Kalapodis (2017) and Kalapodis *et al.* (2018).

Tables 8-12 provide explicit expressions for modal behavior (strength reduction) factors $\bar{q}_k$ for the first four modes and the SP levels of Table 2 as functions of the period T for various types of steel plane EBFs and BRBFs. These tables are restricted to the case of soil class B. Additional tables covering the cases of soil class A, C and D can be found in Kalapodis (2017) and Kalapodis *et al.* (2018), where more details about the whole procedure of constructing modal behavior (strength reduction) factors $\bar{q}_k$ can be also found. For the CP performance level, design equations for $\bar{q}_k$ are omitted even though, one may define them for ξ_k=100% (Papagiannopoulos and Beskos 2011).

It should be stressed that use of modal behavior factors $\bar{q}_k$ instead of just one common behavior factor q for all modes as stipulated in seismic codes, e.g., Eurocode 8 (2009), is certainly a more logical and accurate approach. Computation of displacements, as in the case of the method based on ξ_k, is not needed here since these are automatically satisfied by using $\bar{q}_k$ which are by definition deformation dependent (because they are calculated from ξ_k). Thus, use of the approximate equal displacement rule for displacement determination, as commonly performed in seismic codes, e.g., Eurocode 8 (2009) is avoided.

3. The HFD seismic design method

The third method for performance-based seismic design presented herein is the Hybrid Force/Displacement (HFD) method, which combines the advantages of both FBD and DBD, while at the same time eliminates their disadvantages. Since HFD is also a force-based design method, the main goal here is the construction of a deformation-dependent behavior (or strength reduction) factor q_h that will be used in conjunction with the pseudo-acceleration response/design spectrum to determine the design base shear of the structure. Employing the SP levels of Table 2, Tables 13-17 provide expressions for q_h in terms of the maximum displacement ductility at the top $\mu_{r,\max}$, which in turn is given in terms of the natural period T, number of storeys S, frame height H, and soil class B for the steel plane EBFs and BRBFs considered. Additional tables for the cases of soil classes A, C and D are given in Kalapodis (2017). In order to obtain these expressions, the plane EBFs and BRBFs are designed on the basis of Eurocode 3 (2005) and Eurocode 8 (2009) by means of SAP2000 (2016).

Table 3 ξ_k(%) for EBFs with chevron bracing & intermediate link, soil class B

SP level	Mode 1	Mode 2	Mode 3	Mode 4
SP1-IO	ξ_1 = -0.26T+2.50 (0.20 ≤ T ≤ 1.90)	ξ_2 = -15.12T+4.78 (0.08 ≤ T ≤ 0.25) ξ_2 = -0.62T+1.16 (0.25 ≤ T ≤ 0.64)	ξ_3 = -12.35T+3.54 (0.13 ≤ T ≤ 0.22) ξ_3 = -1.07T+1.06 (0.22 ≤ T ≤ 0.34)	ξ_4 = -33.77T+6.40 (0.09 ≤ T ≤ 0.17) ξ_4 = 0.93T+0.50 (0.17 ≤ T ≤ 0.24)
SP2-DL	ξ_1 = -28.75T+43.75 (0.20 ≤ T ≤ 0.60) ξ_1 = 3.46T+24.42 (0.60 ≤ T ≤ 1.90)	ξ_2 = -3.03T+9.97 (0.32 ≤ T ≤ 0.64)	ξ_3 = -10.00T+10.50 (0.25 ≤ T ≤ 0.34)	ξ_4=100.00 (0.09 ≤ T ≤ 0.24)
SP3-LS	ξ_1 = -30.95T+81.19 (0.20 ≤ T ≤ 0.60) ξ_1 = 62.62 (0.60 ≤ T ≤ 1.90)	ξ_2=100.00 (0.08 ≤ T ≤ 0.64)	ξ_3=100.00 (0.13 ≤ T ≤ 0.34)	ξ_4=100.00 (0.09 ≤ T ≤ 0.24)

Table 4 ξ_k(%) for EBFs with diagonal bracing & intermediate link, soil class B

SP level	Mode 1	Mode 2	Mode 3	Mode 4
SP1-IO	ξ_1 = 0.07T+1.89 (0.20 ≤ T ≤ 1.70)	ξ_2 = -1.76T+1.82 (0.10 ≤ T ≤ 0.55)	ξ_3 = -127.50T+20.02 (0.11 ≤ T ≤ 0.15) ξ_3 = -1.07T+1.06 (0.15 ≤ T ≤ 0.28)	ξ_4 = -3.00T+1.35 (0.15 ≤ T ≤ 0.20)
SP2-DL	ξ_1 = -277.78 T+105.56 (0.20 ≤ T ≤ 0.30) ξ_1 = -4.26T+23.53 (0.30 ≤ T ≤ 1.70)	ξ_2 = -16.67T+16.67 (0.35 ≤ T ≤ 0.55)	ξ_3=100.00 (0.11 ≤ T ≤ 0.28)	ξ_4=100.00 (0.15 ≤ T ≤ 0.20)
SP3-LS	ξ_1 = -4.00T+62.80 (0.20 ≤ T ≤ 1.70)	ξ_2=100.00 (0.10 ≤ T ≤ 0.55)	ξ_3=100.00 (0.11 ≤ T ≤ 0.28)	ξ_4=100.00 (0.15 ≤ T ≤ 0.20)

Table 5 ξ_k(%) for EBFs with chevron bracing & flexural link, soil class B

SP level	Mode 1	Mode 2	Mode 3	Mode 4
SP1-IO	ξ_1 = 0.14T+1.45 (0.30 ≤ T ≤ 1.70)	ξ_2 = -7.75T+2.55 (0.10 ≤ T ≤ 0.25) ξ_2 = 1.14T+0.33 (0.25 ≤ T ≤ 0.60)	ξ_3 = 0.48T+0.43 (0.14 ≤ T ≤ 0.35)	ξ_4 = -1.35T+1.13 (0.09 ≤ T ≤ 0.24)
SP2-DL	ξ_1 = -15.11T+38.14 (0.30 ≤ T ≤ 1.70)	ξ_2 = -30.56T+22.39 (0.35 ≤ T ≤ 0.50) ξ_2 = 29.00T-7.39 (0.50 ≤ T ≤ 0.60)	ξ_3= -104.29T+38.00 (0.23 ≤ T ≤ 0.30) ξ_3= 18.00T+1.31 (0.30 ≤ T ≤ 0.35)	ξ_4=100.00 (0.09 ≤ T ≤ 0.24)
SP3-LS	ξ_1 = -12.23T+71.16 (0.30 ≤ T ≤ 1.70)	ξ_2=100.00 (0.10 ≤ T ≤ 0.60)	ξ_3=100.00 (0.14 ≤ T ≤ 0.35)	ξ_4=100.00 (0.09 ≤ T ≤ 0.24)

Table 6 ξ_k(%) for EBFs with diagonal bracing & flexural link, soil class B

SP level	Mode 1	Mode 2	Mode 3	Mode 4
SP1-IO	ξ_1 = 1.30 (0.22 ≤ T ≤ 1.50)	ξ_2 = -0.81T+1.09 (0.11 ≤ T ≤ 0.48)	ξ_3 = -2.65T+1.40 (0.15 ≤ T ≤ 0.27)	ξ_4 = -9.09T+2.38 (0.12 < T < 0.19)
SP2-DL	ξ_1 = 23.33T+31.33 (0.20 ≤ T ≤ 0.80) ξ_1 = -45.32T+86.25 (0.80 ≤ T ≤ 1.50)	ξ_2 = -30.77T+25.77 (0.32 ≤ T ≤ 0.48)	ξ_3= 2.00T+13.06 (0.23 ≤ T ≤ 0.27)	ξ_4=100.00 (0.12 ≤ T ≤ 0.19)
SP3-LS	ξ_1 = 13.95T+64.65 (0.20 ≤ T ≤ 1.10) ξ_1 = -60.77T+146.85 (1.10 ≤ T ≤ 1.50)	ξ_2=100.00 (0.11 ≤ T ≤ 0.48)	ξ_3=100.00 (0.15 ≤ T ≤ 0.27)	ξ_4=100.00 (0.12 ≤ T ≤ 0.19)

Table 7 ξ_k(%) for BRBFs with chevron bracing, soil class B

SP level	Mode 1	Mode 2	Mode 3	Mode 4
SP1-IO	ξ_1 = -3.33T+2.77 (0.22 ≤ T ≤ 0.50) ξ_1 = 0.40T+0.90 (0.50 ≤ T ≤ 1.50)	ξ_2 = -16.67T+3.83 (0.11 ≤ T ≤ 0.17) ξ_2 = -1.27T+1.22 (0.17 ≤ T ≤ 0.48)	ξ_3 = -4.60T+1.57 (0.10 ≤ T ≤ 0.27)	ξ_4 = -6.51T+2.03 (0.11 ≤ T ≤ 0.19)
SP2-DL	ξ_1 = -38.16T+51.16 ≤ T ≤ 1.00) ξ_1 = 9.61T+3.39 ≤ T ≤ 1.50)	ξ_2 = -54.29T+29.95 ≤ T ≤ 0.42) ξ_2 = 57.33T -16.93 ≤ T ≤ 0.48)	ξ_3= -5.44T+9.97 . ≤ T ≤ 0.27)	ξ_4=100.00 1 ≤ T ≤ 0.19)
SP3-LS	ξ_1 = 28.57T+62.24 (0.22 ≤ T ≤ 0.50) ξ_1 = -26.53T+89.80 (0.50 ≤ T ≤ 1.50)	ξ_2=100.00 (0.11 ≤ T ≤ 0.48)	ξ_3=100.00 (0.10 ≤ T ≤ 0.27)	ξ_4=100.00 (0.11 ≤ T ≤ 0.19)

Table 8 $\bar{q}_k$ for EBFs with chevron bracing & intermediate link, soil class B

SP level	Mode 1	Mode 2	Mode 3	Mode 4
SP1-IO	$\bar{q}_k$=1 (0.20 ≤ T ≤ 1.90)	$\bar{q}_k$=1 (0.08 ≤ T ≤ 0.64)	$\bar{q}_k$=1 (0.13 ≤ T ≤ 0.34)	$\bar{q}_k$=1 (0.09 ≤ T ≤ 0.24)
SP2-DL	$\bar{q}_k$=0.24T^2+0.52T+1.99 (0.20 ≤ T ≤ 1.90)	$\bar{q}_k$=0.07T + 1.22 (0.32 ≤ T ≤ 0.64)	$\bar{q}_k$=6.52T + 1.64 (0.25 ≤ T ≤ 0.34)	$\bar{q}_k$=4.20T + 2.18 (0.09 ≤ T ≤ 0.24)
SP3-LS	$\bar{q}_k$=-0.74T^2+1.65T+ 2.70 (0.20 ≤ T ≤ 1.90)	$\bar{q}_k$=10.4T^2+10.56T+1.36 (0.08 ≤ T ≤ 0.64)	$\bar{q}_k$=6.52T + 1.64 (0.13 ≤ T ≤ 0.34)	$\bar{q}_k$=4.20T + 2.18 (0.09 ≤ T ≤ 0.24)

Table 9 $\bar{q}_k$ for EBFs with diagonal bracing & intermediate link, soil class B

SP level	Mode 1	Mode 2	Mode 3	Mode 4
SP1-IO	$\bar{q}_k$=1 (0.20 ≤ T ≤ 1.70)	$\bar{q}_k$=1 (0.10 ≤ T ≤ 0.55)	$\bar{q}_k$=-0.18T + 1.04 (0.11 ≤ T ≤ 0.28)	$\bar{q}_k$=1 (0.15 ≤ T ≤ 0.20)
SP2-DL	$\bar{q}_k$=-1.10T^3+3.11T^2-2.72T+2.65 (0.20 ≤ T ≤ 1.70)	$\bar{q}_k$=-0.73T + 1.66 (0.35 ≤ T ≤ 0.55)	$\bar{q}_k$=8.35T + 1.24 (0.11 ≤ T ≤ 0.28)	$\bar{q}_k$=9.89T + 1.09 (0.15 ≤ T ≤ 0.20)
SP3-LS	$\bar{q}_k$=-1.40T^2+2.74T+2.13 (0.20 ≤ T ≤ 1.70)	$\bar{q}_k$=-26.18T^2 + 26.69T-0.84 (0.10 ≤ T ≤ 0.55)	$\bar{q}_k$=8.35T + 1.24 (0.11 ≤ T ≤ 0.28)	$\bar{q}_k$=9.89T + 1.09 (0.15 ≤ T ≤ 0.20)

Table 10 $\bar{q}_k$ for EBFs with chevron bracing & flexural link, soil class B

SP level	Mode 1	Mode 2	Mode 3	Mode 4
SP1-IO	$\bar{q}_k$=1 (0.30 ≤ T ≤ 1.70)	$\bar{q}_k$=1 (0.10 ≤ T ≤ 0.60)	$\bar{q}_k$=1 (0.14 ≤ T ≤ 0.35)	$\bar{q}_k$=1 (0.09 ≤ T ≤ 0.24)
SP2-DL	$\bar{q}_k$=-0.49T^2+0.42T+2.14 (0.30 ≤ T ≤ 1.70)	$\bar{q}_k$=81.80T^3-106.60T^2+43.90T - 4.34 (0.35 ≤ T ≤ 0.60)	$\bar{q}_k$=-1.73T + 1.99 (0.23 ≤ T ≤ 0.35)	$\bar{q}_k$=4.20T + 2.18 (0.09 ≤ T ≤ 0.24)
SP3-LS	$\bar{q}_k$=1.86T^3 - 7.08T^2+7.39T+1.46 (0.30 ≤ T ≤ 1.70)	$\bar{q}_k$=-14.85T^2+14.10T+0.69 (0.10 ≤ T ≤ 0.60)	$\bar{q}_k$=6.52T + 1.64 (0.14 ≤ T ≤ 0.35)	$\bar{q}_k$=4.20T + 2.18 (0.09 ≤ T ≤ 0.24)

Table 11 $\bar{q}_k$ for EBFs with diagonal bracing & flexural link, soil class B

SP level	Mode 1	Mode 2	Mode 3	Mode 4
SP1-IO	$\bar{q}_k$=1 (0.20 ≤ T ≤ 1.50)	$\bar{q}_k$=1 (0.11 ≤ T ≤ 0.48)	$\bar{q}_k$=1 (0.11 ≤ T ≤ 0.27)	$\bar{q}_k$=1 (0.10 ≤ T ≤ 0.19)
SP2-DL	$\bar{q}_k$=-2.34T^2 +3.78T+1.30 (0.20 ≤ T ≤ 1.50)	$\bar{q}_k$=-0.85T + 1.84 (0.35 ≤ T ≤ 0.48)	$\bar{q}_k$=0.80T + 1.19 (0.23 ≤ T ≤ 0.27)	$\bar{q}_k$=9.89T + 1.29 (0.10 ≤ T ≤ 0.19)
SP3-LS	$\bar{q}_k$=-3.28T^3+5.65T^2-1.13T+2.93 (0.20 ≤ T ≤ 1.50)	$\bar{q}_k$=-30.51T^2 + 25.83T-1.39 (0.11 ≤ T ≤ 0.48)	$\bar{q}_k$=2.80T + 2.66 (0.11 ≤ T ≤ 0.27)	$\bar{q}_k$=9.89T + 1.29 (0.10 ≤ T ≤ 0.19)

Table 12 $\bar{q}_k$ for BRBFs with chevron bracing, soil class B

SP level	Mode 1	Mode 2	Mode 3	Mode 4
SP1-IO	$\bar{q}_k$=1 (0.20 ≤ T ≤ 1.50)	$\bar{q}_k$=1 (0.11 ≤ T ≤ 0.48)	$\bar{q}_k$=1 (0.10 ≤ T ≤ 0.27)	$\bar{q}_k$=1 (0.11 ≤ T ≤ 0.19)
SP2-DL	$\bar{q}_k$=1.23T^3 - 3.00T^2+1.54T+1.99 (0.20 ≤ T ≤ 1.50)	$\bar{q}_k$=168.01T^3 - 175.41T^2 + 58.18T - 4.77 (0.25 ≤ T ≤ 0.48)	$\bar{q}_k$= -14.36T^2 + 5.63T + 0.72 (0.18 ≤ T ≤ 0.27)	$\bar{q}_k$=16.93T+ 0.08 (0.11 ≤ T ≤ 0.19)
SP3-LS	$\bar{q}_k$=-2.55T^2 +4.41T+1.90 (0.20 ≤ T ≤ 1.50)	$\bar{q}_k$=3.72T + 2.42 (0.11 ≤ T ≤ 0.48)	$\bar{q}_k$=6.91T + 1.57 (0.10 ≤ T ≤ 0.27)	$\bar{q}_k$=16.93T+ 0.08 (0.11 ≤ T ≤ 0.19)

Table 13 q_h for EBFs with chevron bracing & intermediate link, soil class B

SP level	Strength reduction factor (q_h)	maximum roof ductility ($\mu_{r,max}$)	Range of the first natural period *(T)*
SP1-IO	1 + 4.54(μ$_r$ -1)$^{0.057}$	0.77(T$^{0.034}$)(S$^{-0.689}$)(H$^{0.544}$)	0.20 ≤ T ≤ 1.90
SP2-DL	1 + 1.71(μ$_r$ -1)$^{0.295}$	1.12(T$^{-0.167}$)(S$^{-0.117}$)(H$^{0.315}$)	
SP3-LS	1 + 2.96(μ$_r$ -1)$^{0.194}$	1.49(T$^{-0.245}$)(S$^{-0.356}$)(H$^{0.519}$)	
SP4-CP	1 + 4.54(μ$_r$ -1)$^{0.057}$	2.50(T$^{-0.109}$)(S$^{-0.728}$)(H$^{0.703}$)	
Roof displacement at first yield: $u_{r,y}$ = 0.002(T$^{-0.527}$)(S$^{0.850}$)(H$^{0.537}$)			

Table 14 q_h for EBFs with diagonal bracing & intermediate link, soil class B

SP level	Strength reduction factor (q_h)	maximum roof ductility ($\mu_{r,max}$)	Range of the first natural period *(T)*
SP1-IO	$1 + 0.26(\mu_r - 0.5)^{2.524}$	$0.02(T^{-1.315})(S^{0.399})(H^{0.847})$	
SP2-DL	$1 + 1.63(\mu_r - 1)^{0.292}$	$8.26(T^{0.665})(S^{-0.859})(H^{0.242})$	$0.20 \leq T \leq 1.70$
SP3-LS	$1 + 2.38(\mu_r - 1)^{0.372}$	$20.98(T^{0.891})(S^{-1.110})(H^{0.268})$	
SP4-CP	$1 + 2.94(\mu_r - 1)^{0.312}$	$22.88(T^{0.955})(S^{-1.590})(H^{0.641})$	
Roof displacement at first yield: $u_{r,y} = 0.046(T^{0.928})(S^{-0.217})(H^{0.293})$			

Table 15 q_h for EBFs with chevron bracing & flexural link, soil class B

SP level	Strength reduction factor (q_h)	maximum roof ductility ($\mu_{r,max}$)	Range of the first natural period *(T)*
SP1-IO	$1 + 2.0(\mu_r - 0.5)^{6.700}$	$0.13(T^{-0.971})(S^{-0.055})(H^{0.612})$	
SP2-DL	$1 + 1.68(\mu_r - 1)^{0.486}$	$1.35(T^{-0.249})(S^{-0.183})(H^{0.287})$	$0.30 \leq T \leq 1.70$
SP3-LS	$1 + 3.05(\mu_r - 1)^{0.241}$	$1.01(T^{-0.738})(S^{0.046})(H^{0.380})$	
SP4-CP	$1 + 4.92(\mu_r - 1)^{0.095}$	$1.92(T^{-0.341})(S^{-0.562})(H^{0.720})$	
Roof displacement at first yield: $u_{r,y} = 0.003(T^{-0.474})(S^{0.721})(H^{0.518})$			

Table 16 q_h for EBFs with diagonal & flexural link, soil class B

SP level	Strength reduction factor (q_h)	maximum roof ductility ($\mu_{r,max}$)	Range of the first natural period *(T)*
SP1-IO	$1 + 0.31(\mu_r - 0.5)^{1.664}$	$0.07(T^{-1.268})(S^{0.090})(H^{0.752})$	
SP2-DL	$1 + 1.78(\mu_r - 1)^{0.337}$	$2.66(T^{0.223})(S^{-0.422})(H^{0.299})$	$0.22 \leq T \leq 1.50$
SP3-LS	$1 + 1.96(\mu_r - 1)^{0.595}$	$1.45(T^{-0.319})(S^{-0.094})(H^{0.383})$	
SP4-CP	$1 + 1.24(\mu_r - 1)^{0.629}$	$1.80(T^{-0.167})(S^{-0.544})(H^{0.757})$	
Roof displacement at first yield: $u_{r,y} = 0.083(T^{1.563})(S^{-0.164})(H^{0.106})$			

Table 17 q_h for BRBFs with chevron bracing, soil class B

SP level	Strength reduction factor (q_h)	maximum roof ductility ($\mu_{r,max}$)	Range of the first natural period *(T)*
SP1-IO	$1 + 0.41(\mu_r - 0.5)^{4.162}$	$0.69(T^{-0.188})(S^{-0.704})(H^{0.551})$	
SP2-DL	$1 + 1.69(\mu_r - 1)^{0.280}$	$2.42(T^{0.181})(S^{-0.633})(H^{0.419})$	$0.20 \leq T \leq 1.50$
SP3-LS	$1 + 3.24(\mu_r - 1)^{0.075}$	$6.23(T^{0.404})(S^{-0.860})(H^{0.452})$	
SP4-CP	$1 + 4.70(\mu_r - 1)^{0.005}$	$9.82(T^{0.628})(S^{-1.301})(H^{0.745})$	
Roof displacement at first yield: $u_{r,y} = 1.9 \cdot 10^{-4}(T^{-1.337})(S^{1.539})(H^{0.657})$			

After the dimensioning of structural members, the frames are modeled in detail and subjected to numerous non-linear time history/incremental dynamic analyses (NLTH/IDA) via the Ruaumoko 2D (Carr 2007) software, incorporating 100 far-field seismic excitations, appropriately scaled to drive the frames to specific target performance/damage levels. A frame reaches a target performance/damage level right after a dissipative structural member develops maximum permitted local ductility, or when maximum IDR of a frame is equal to certain target limits according to SEAOC (1999). Thus, through these NLTH/IDA analyses a response databank is obtained. Then, by means of non-linear regression analysis, three different types of empirical relations are provided in Tables 13-17. More specifically, the first expression estimates the roof first yield displacement $u_{r,y}$ as a function of *T(sec), S* and *H(m)*, the second expression evaluates the maximum roof ductility $\mu_{r,\max}$ as a function of the same parameters as in $u_{r,y}$ and the third relation provides the behavior (strength reduction) factor *(q_h)* as a function of the maximum roof displacement ductility $\mu_{r,\max}$.

In the next three sections details are provided about the design of the considered frames and the seismic motions and modeling of these frames for the nonlinear dynamic analyses needed for the creation of the aforementioned response databank.

4. Design of frames considered

EBFs with diagonal and chevron bracing configurations (Fig. 1) and BRBFs with chevron bracing configuration (Fig. 2, left) are designed according to Eurocode 3 (2005) and Eurocode 8 (2009) using SAP2000 (2016), considering a peak ground acceleration (PGA) equal to 0.24 g, soil class B and behavior (strength reduction) factor q=4 which accounts for medium ductility class. Since BRBFs are not yet included in Eurocodes, their design is accomplished as suggested in Bosco *et al.* (2015), i.e., by modifying the rules provided by Eurocode 8 (2009) regarding steel concentrically braced frames.

The EBFs and the BRBFs are designed for two stiffness levels (different sections for beams and columns) and have seven different height levels (as expressed by the number of storeys). The EBFs may have three types of links: a shear link (X=0.5 m), or an intermediate (X=1.0 m) or a flexural link (X=1.5 m), (see Table 1 and Fig. 1). Hence, this study includes 84 different EBFs (7 height levels×3 link types×2 stiffness levels×2 frame configurations) and 14 different BRBFs (7 height levels×2 stiffness levels). The steel grade used is S275 for both EBFs and BRBFs.

The design load combination considered includes dead (G) and live (Q) loads and reads as follows: G+0.3Q=27.5 kN/m. The chosen section types for the steel members of the EBFs, are IPE, HEB and CHS for beams, columns and braces respectively. For the steel members of the BRBFs, the only difference with EBFs is that the brace sections are modelled by a rectangular section (steel core in Fig. 2, right). Additionally, beam-column connections are considered as moment resisting ones and column sections are oriented so that their strong axis is perpendicular to the plane of the frame. Beams do not exhibit lateral-torsional buckling because of the presence of a composite slab. The sections of the designed frames as well as the period of their first mode of vibration are shown in Tables 18-19. Sections for the cases of EBFs having intermediate and shear links are not presented herein due to space limitations and one can consult Kalapodis *et al.* (2018) for them.

As mentioned above, the geometric and the strength characteristics of the seismic links determine the seismic performance of EBFs (Qi *et al.* 2017). According to Eurocode 8 (2009), the behavior of these links can be either flexural (long links that fail due to bending moment), shear (short links that fail due to shear force) or a combination of the two (intermediate links that fail due to bending moment and shear force). Taking into account this difference in the behavior of these links, the group of the 84 EBFs is separated into three groups that include 28 frames each according to the aforementioned link characteristics.

5. Seismic motion selection for nonlinear dynamic analyses

The seismic performance of steel braced frames subjected to near-fault seismic motions has been already investigated by Eskandari and Vafaei (2015). Herein, the 98 frames mentioned in section 4, are subjected to a set of 100 far-field seismic motions, in order to perform extensive parametric studies involving nonlinear dynamic analyses (NLDA), with the aid of Ruaumoko 2D (Carr 2007). These far-field seismic motions are selected from the PEER database (2013) and are separated into four groups. Each group represents a certain soil class, i.e., A, B, C or D following the soil categorization of Eurocode 8 (2009). The seismic motions belonging to soil class B along with other data such as PGA (peak ground acceleration) values, the names of the recording stations and the components of the recordings as well as the date of the earthquake event, are listed in Table 20. One can consult Kalapodis (2017) for the seismic motions of the rest three soil classes (soil classes A, C and D).

The selection of these 100 seismic motions is based on certain criteria: i) the magnitude and the effective duration of the earthquake range from 5.2 to 7.7 and from 7.0 to 45.0 sec, respectively; ii) the distance between the recording station and the fault is between 20.0 and 40.0 km. Due to its wide use, PGA is used herein to represent the seismic intensity for purposes of IDA. In particular, in order to obtain the targeted performance/damage levels (expressed by the IDR and μ_θ, μ_δ values of Table 2), a recurrent IDA process, utilizing Ruaumoko 2D (Carr 2007) and Matlab (2015), is implemented permitting thus the evaluation of the pertinent scale factor (SF). Each SF found corresponds to a specific combination of a steel braced frame, a seismic motion and a performance/damage level. Hence, multiplication of seismic motion by this SF leads to a resulting motion that essentially forces the structure to reach the performance/damage level that the SF by the aforementioned computation process satisfies. The maximum SF value found herein is 4, and complies with the upper limit of the SF mandated by ASCE (2017). The upper values for the performance/damage levels of EBFs are provided in Table 2.

It should be reminded that for the case of BRBFs there is no a complete study in literature that relates IDR with the axial displacement of the buckling restrained brace (BRB) for various performance levels. Thus, it is decided herein to use for the BRBFs the IDR limits of Table 2 that hold for EBFs. Moreover, for the IDR values corresponding to the performance levels SP3-LS and SP4-CP of Table 2, it is checked if the axial displacement of the BRB is larger than two times the horizontal displacement of the steel braced frame caused by the aforementioned IDR values (Bosco *et al.* 2015).

6. Structural modeling for nonlinear dynamic analyses

An elaborate modeling of the frames, necessary to perform the nonlinear dynamic analyses by using Ruaumoko 2D (Carr 2007), is briefly presented in the following. For more details, one can consult Kalapodis (2017). The influence of the concrete slab is taken into account through the consideration of a diaphragm action at every floor. Large deformation effects are also taken into account. Beam members including the flexural and the intermediate link members are modeled utilizing the Giberson mode (Carr 2007), which incorporates two rotational springs (to account for plastic hinges) at both ends. According to this model, the interaction between bending moment and axial force is neglected. Shear link members are modelled employing an enhanced version of the Giberson beam model. More specifically, two translational springs are added at both ends of these link

Table 18 Designed BRBFs

Frame	Storey	Frame sections: HEB (columns) - IPE (beams) - Steel core (BRB)	Period (sec)
1	2	240-300-15.4(1-2)	0.244
2	2	220-300-15.4(1), 220-300-14.0(2)	0.250
3	3	260-360-26.6(1), 260-330-18.9(2), 240-300-15.4(3)	0.288
4	3	240-330-26.6(1), 240-330-18.9(2), 220-300-15.4(3)	0.292
5	6	400-400-40.6(1), 400-400-33.6(2), 320-360-26.6(3-4), 260-360-21.0(5), 260-330-14.0(6)	0.485
6	6	360-360-40.6(1), 360-360-33.6(2), 300-360-26.6(3), 300-330-26.6(4), 240-330-21.0(5), 240-330-14.0(6)	0.502
7	9	550-500-40.6(1-2), 450-500-33.6(3), 400-450-33.6(4), 360-400-26.6(5-6), 300-400-21.0(7-8), 240-400-18.9(9)	0.694
8	9	500-450-40.6(1), 450-450-33.6(2-3), 400-450-26.6(4-5), 300-400-21(6-7), 260-400-16.1(8), 220-360-15.4(9)	0.740
9	12	650-550-40.6(1-2), 600-500-33.6(3-4), 500-450-33.6(5-6), 400-400-26.6(7-8), 360-400-21(9-10), 300-360-17.5(11-12)	0.966
10	12	600-500-40.6(1-2), 550-500-33.6(3-4), 450-450-26.6(5-6), 360-400-21.0(7-8), 300-400-18.9(9), 260-360-17.5(10-12)	1.030
11	15	800-550-40.6(1-2), 700-500-33.6(3-4), 600-500-26.6(5-6), 500-450-26.6(7-8), 450-400-21(9-11), 400-360-18.9(12-13), 320-360-17.5(14), 320-360-16.1(15)	1.246
12	15	700-550-40.6(1-2), 650-500-33.6(3-5), 500-450-26.6(6-8), 400-400-21.0(9-10), 360-360-21(11-13), 300-330-17.5(14-15)	1.294
13	17	800-550-40.6(1-4), 700-500-33.6(5-6), 600-450-33.6(7-8), 500-400-26.6(9-10), 450-360-21(11-13),400-360-18.9(14-15), 360-330-17.5(16-17)	1.457
14	17	800-550-40.6(1-2), 700-500-33.6(3-4), 600-450-33.6(5-6), 500-400-26.6(7-9), 400-400-21.0(10-12),360-360-18.9(13-14), 300-330-17.5(15-16), 260-330-14.0(17)	1.501

Note: 280/300-270-16.9(5-6) indicates that sections at storeys 5 and 6 have as follows: HE300B for interior columns, HE280B for exterior columns, IPE270 for beams and 16.9 cm^2 is the area of the rectangular steel core. For the case of identical interior and exterior columns, e.g., HE300B, one has 300-270-16.9(5-6)

members in order to consider their shear behavior (Caprili *et al.* 2018). Bracing members are also modelled by using the aforementioned Giberson model (Carr 2007), incorporating elastic hinges at their ends. A beam-column model that takes includes the interaction between bending moment and axial force (Carr 2007), is used to model the columns of the steel frames.

Regarding the BRBs, there is a variety of models for the simulation of their nonlinear behavior, e.g., the one described in Bosco *et al.* (2015). In the present work, use of the Giberson beam model that includes elastic hinges at both ends of the BRB is made. All frame members obey to a bilinear hysteretic rule, with a value of bilinear factor equal to 0.012 for the brace members, to 0.03 for the beam and column members and to 0.02 for the BRBs.

Even though some hysteretic models include stiffness and strength degradation effects, these effects are omitted for the purposes of the present work. The main reason behind their omission is the very high computational demands associated with the numerous non-linear dynamic analyses of steel braced frames having different bracing and link configurations and being subjected to a large number of seismic motions. On the other hand, the influence of these effects on the seismic behavior of EBFs and BRBFs seems to be insignificant (Kazemzadeh and Topkaya 2017), while in some cases, the inclusion of such effects, may lead to discrepancies between analysis results and experiments (Gleise and Koboevic 2014).

Regarding EBFs, there is a consideration of rigid horizontal, vertical and diagonal segments upon members that intersect in the connection areas, with a view to include both the effects of member eccentricity from the centroidal axes and of the gusset plate, into the frame modeling (Hsiao *et al.* 2012). At first, dimensioning of gusset plates is performed following the capacity design principles (Hsiao *et al.* 2012, Okazaki *et al.* 2013). The combination of frame design according to Eurocode 8 (2009) with the capacity design of gusset plates, aims to the exhibition of first yield strictly to the links of the EBFs and to the BRBs of the BRBFs. After dimensioning the gusset plates, modelling of the aforementioned rigid segments follows Hsiao *et al.* (2012). Finally, for the case of BRBFs, the BRBs are considered pinned and hence, the rigid links are associated only with the geometric properties of the intersected members (beam/brace/column).

Modelling of the panel zone is performed only when gusset plates are not a part of a connection. The behavior of the panel zone can be successfully represented by the "scissors model" (Carr 2007) which consists of an equivalent zero-length rotational spring that sufficiently represents its deformation in shear. In particular, such model incorporates two nodes having the same coordinates and being located at the intersection point of the centroidal axes of a column and beam. A trilinear law that relates moment-rotation (M-θ) is utilized to describe the nonlinear behavior of the "scissor model". The validity of this trilinear law has been confirmed via comparisons involving several experiments and employed in several studies, e.g.,

Table 19 Designed EBFs with flexural links (X=1.5 m)

Frame	Storey	Frame sections: HEB (columns) - IPE (beams) - CHS (braces)	Period (sec)
1a	2	240-300-152.4x4(1.2)	0.336
2a	2	200-300-139.7x4(1-2)	0.348
3a	3	260-330-193.7x4.5(1), 240-300-193.7x4.5(2),240-300-168.3x4 (3)	0.414
4a	3	240-300-193.7x4.5(1), 240-270-168.3x4(2-3)	0.456
5a	6	340-360-219.1x5(1-2), 300-300-193.7x4.5(3-4), 260-270-193.7x4.5(5), 260-270-168.3x4(6)	0.700
6a	6	300-360-219.1x5(1-2), 260-300-193.7x4.5(3-4), 240-270-168.3x4(5-6)	0.720
7a	9	450-400-244.5x5.4(1), 400-360-244.5x5.4(2-3), 340-330-219.1x5(4-6), 300-300-193.7(7), 260-270-168.3x4(8-9)	0.931
8a	9	450-400-219.1x5(1), 400-360-219.1x5(2-3), 340-330-193.7x4.5(4-5), 300-300-193.7(6-7), 260-270-168.3x4(8-9)	0.976
9a	12	550-450-244.5x5.4(1), 500-450-244.5x5.4(2-3), 450-400-219.1x5(4-5), 400-360-219.1x5(6-7), 360-360-193.7x4(8-9), 300-300-168.3x4(10-12)	1.123
10a	12	500-400-219.5x5(1), 450-400-219.5x5(2-3), 400-360-193.7x4.5(4-5), 360-330-193.7x4.5 (6-7), 300-300-193.7 x4.5(8-9), 260-300-193.7x4.5(10), 260-270-168.3x4(11-12)	1.289
11a	15	650-450-244.5x5.4(1), 600-450-244.5x5.4(2), 550-400-244.5 x5.4(3-4), 500-360-219.1x5 (5-6), 450-330-193.7x4.5(7-8), 400-330-19.7x4.5(9-10), 360-300-19.7x4.5(11-12), 320-300-168.3x4(13), 280-270-168.3x4(14-15)	1.520
12a	15	600-450-219.1x5(1), 550-400-219.1x5(2-3), 500-360-193.7x 4.5(4-5), 450-360-193.7x4.5 (6-7), 400-330-193.7x4.5(8-9), 360-300-193.7x4.5(10-11), 320-300-193.7 x4.5(12-13), 280-270-168.3x4(14-15)	1.570
13a	17	700-450-244.5x5.4(1-2), 650-400-244.5x5.4(3-4), 600-400- 219.1x5(5-6), 500-360-219.1x5(7-9), 400-330-193.7x4.5(10-12), 360-300-193.7x4.5(13-15), 300-270-193.7x4.5(16-17)	1.669
14a	17	700-450-244.5x5.4(1), 600-400-244.5x5.4(2-3), 550-400-219 x5(4-5), 450-360-193.7x4.5(6-7), 400-360-193.7x4.5(8-9), 360-330-193.7x4.5(10-11), 320-360-193.7x4.5(12-13), 280-330-168.3x4(14-15), 260-270-168.3x4(16-17)	1.731
15b	2	220-300-168.3x4(1-2)	0.242
16b	2	200-300-139.7x4(1-2)	0.274
17b	3	260-300-219.1x5(1), 240-300-193.7x4.5(2-3)	0.327
18b	3	240-300-193.7x4.5(1), 240-300-168.3x4(2-3)	0.344
19b	6	400-330-219.1x5(1-2), 340-300-219.1x5(3-4), 280-270-193.7x4.5(5-6)	0.524
20b	6	360-330-193.7x4.5(1-2), 320-300-193.7x4.5(3-4), 260-300-168.3x4(5-6)	0.558
21b	9	450-360-219.1x5(1-2), 400-360-219.1x5(3-4), 360-330- 193.7x4.5(5-6), 300-300-168.3(7-8), 260-300-168.3x4(9)	0.748
22b	9	400-360-193.7x4.5(1-2), 360-360-193.7x4.5(3-4), 300-330-168.3x4(5-6), 280-300-168.3x4(7-8), 260-300-168.3x4(9)	0.798
23b	12	500-400-244.5x5.4(1-2), 450-360-219.1x5(3-4), 400-330-219.1x5(5-6), 360-330-193.7x4.5 (7-8), 320-300-193.7x4.5(9-10), 280-300-193.7x4.5(11), 280-300-168.3x4(12)	1.012
24b	12	450-400-219.1x5(1-2), 400-360-219.1x5(3-4), 360-330- 193.7x4.5(5-6), 320-330-193.7x4.5(7-8), 280-300-193.7 x4.5(9-10), 260-300-168.3x4	1.070
25b	15	600-400-244.5x5.4(1-2), 550-360-244.5x5.4(3-4), 500-360-219.1x5(5-6), 450-330-219.1x5 (7-8), 400-330-219.1x5(9-10), 360-193.7x4.5(11-12), 320-300-193.7x4.5(13.14), 280-300-168.3x4(15)	1.242
26b	15	550-400-219.1x5(1-2), 500-360-219.1x5(3-4), 450-360-193.7x4.5(5-6), 400-330-193.7x4.5 (7-8), 360-330-193.7 x4.5(9-10), 320-330-168.3x4(11-12), 280-300-168.3x4(13-15)	1.310
27b	17	700-400-244.5x5.4(1-2), 600-400-244.5x5.4(3-4), 550-360-244.5x5.4(5-6), 500-360-219.1x5 (7-8), 450-330-219.1x5(9-10), 400-330-193.7x4.5(11-12), 360-330-193.7x4.5(13-14), 320-300-193.7x4.5(15-16), 280-300-168.3x4(17)	1.403
28b	17	650-400-219.1x5(1-2), 550-400-219.1x5(3-4), 500-360219.1 x5(5-6), 450-360-193.7x4.5(7-8), 400-330-193.7x4.5(9-10), 360-330-193.7x4.5(11-12), 320-330-168.3x4(13-14), 280-300-168.3x4(15-17)	1.463

Note: Symbols a and b accounts for chevron and diagonal bracing, respectively

Lee *et al.* (2005). The “scissors model” is selected in this work for reasons of simplicity and lower computational sources, compared to more detailed and sophisticated models.

7. Design examples

Three design examples are presented in order to highlight the accuracy of the three considered herein

Table 20 Seismic motions belonging to soil class B

No.	Date	Record name	Comp.	Station name	PGA(g)
1	1992/04/25	Cape Mendocino	NS	89509 Eureka	0.154
2	1992/04/25	Cape Mendocino	EW	89509 Eureka	0.178
3	1980/06/09	Victoria, Mexico	N045	6604 Cerro Prieto	0.621
4	1980/06/09	Victoria, Mexico	N135	6604 Cerro Prieto	0.587
5	1992/04/25	Cape Mendocino	EW	89324 Rio Dell Overpass	0.385
6	1992/04/25	Cape Mendocino	NS	89324 Rio Dell Overpass	0.549
7	1978/08/13	Santa Barbara	N048	283 Santa Barbara Courthouse	0.203
8	1978/08/13	Santa Barbara	N138	283 Santa Barbara Courthouse	0.102
9	1999/09/20	Chi-Chi, Taiwan	NS	TCU095	0.712
10	1999/09/20	Chi-Chi, Taiwan	NS	TCU095	0.378
11	1979/08/06	Coyote Lake	N213	1377 San Juan Bautista	0.108
12	1979/08/06	Coyote Lake	N303	1377 San Juan Bautista	0.107
13	1994/01/17	Northridge	NS	90021 LA – N Westmoreland	0.361
14	1994/01/17	Northridge	EW	90021 LA – N Westmoreland	0.401
15	1986/07/08	N. Palm Springs	NS	12204 San Jacinto – Soboba	0.239
16	1986/07/08	N. Palm Springs	EW	12204 San Jacinto – Soboba	0.250
17	1970/09/12	Lytle Creek	N115	290 Wrightwood	0.162
18	1970/09/12	Lytle Creek	N205	290 Wrightwood	0.200
19	1989/10/18	Loma Prieta	NS	58065 Saratoga – Aloha Ave	0.324
20	1989/10/18	Loma Prieta	EW	58065 Saratoga – Aloha Ave	0.512
21	1992/06/28	Landers	NS	22170 Joshua Tree	0.284
22	1992/06/28	Landers	EW	22170 Joshua Tree	0.274
23	1976/09/15	Friuli, Italy	NS	8014 Forgaria Cornino	0.212
24	1976/09/15	Friuli, Italy	EW	8014 Forgaria Cornino	0.260
25	1999/09/20	Chi-Chi, Taiwan	N045	TCU045	0.512

Table 21 Results obtained by NLDA and by spectrum analysis of Eurocode 8 (2009)

	Motion	Base shear (kN)	IDR$\leq$ 0.022	D_{top} (m)	θ_{link} (rad$\cdot 10^{-3}$)$\leq$ 0.02	$\mu_{\theta}\leq$ 6.2
Non-linear dynamic analysis	1	393.66	0.0071	0.094	19.09	2.56
	2	391.54	0.0078	0.109	20.74	2.68
	3	379.70	0.0066	0.095	18.46	2.39
	4	372.88	0.0058	0.085	16.84	2.11
	5	384.71	0.0078	0.107	20.25	2.61
	6	375.86	0.0071	0.094	18.87	2.43
	7	378.29	0.0072	0.092	20.41	2.68
	8	377.35	0.0081	0.105	22.61	2.96
	9	320.80	0.0082	0.114	21.89	2.82
	10	352.67	0.0081	0.090	19.22	2.93
	Mean values	372.75	0.0074	0.099	19.84	2.62
Spectrum analysis of Eurocode 8		376.96	0.0069	0.114		

seismic design methods and also to compare their results with those of the seismic design based on Eurocode 8 (2009). More specifically, the first numerical example refers to the seismic design of a seven-storey plane steel EBF having diagonal bracings (Fig. 1, right) and flexural links, for the life safety (LS) performance level. The second example refers to the seismic design of a seven-storey steel plane BRBF for a targeted IDR=0.022. Finally, the third example presents the seismic design of a five-storey EBF having chevron bracings and intermediate links for the four seismic performance levels of Table 2. The validity of the aforementioned seismic designs is then verified by non-linear dynamic analyses, using ten seismic motions compatible to the elastic design spectrum of Eurocode 8 (2009).

7.1 EBF with flexural links

A seven-storey steel plane EBF having diagonal bracings and flexural links is designed according to Eurocode 3 (2005) and Eurocode 8 (2009) with the aid of SAP2000 (2016). This EBF has 3 bays of 5.0 m length each, while the height of each storey is equal to 3.0 m. The steel grade is S275. HEB, IPE and CHS section types are

Table 22 Results obtained by NLDA and by spectrum analysis using the ξ_k and $\bar{q}_k$ methods

	Motion	Base shear (kN)	IDR≤0.022	D_{top} (m)	θ_{link}(rad·10^{-3})≤ 0.02	μ_θ≤ 6.2
Non-linear dynamic analysis	1	405.51	0.0062	0.086	17.25	2.08
	2	409.29	0.0068	0.100	19.54	2.41
	3	409.11	0.0061	0.090	19.82	2.27
	4	374.20	0.0053	0.079	17.64	2.04
	5	363.66	0.0070	0.101	16.46	2.42
	6	405.13	0.0067	0.090	17.97	2.33
	7	405.82	0.0062	0.082	20.55	2.36
	8	406.57	0.0076	0.097	24.33	2.82
	9	335.61	0.0077	0.111	18.73	2.71
	10	405.93	0.0065	0.080	18.76	2.39
	Mean values	392.08	0.0066	0.092	19.11	2.38
Spectrum analysis using ξ_k method		387.70				
Spectrum analysis using $\bar{q}_k$ method		389.30				

Table 23 Results obtained by NLDA and by spectrum analysis using the HFD method

	Motion	Base shear (kN)	IDR≤ 0.022	D_{top} (m)	θ_{link}(rad·10^{-3})≤0.02	μ_θ≤6.2
Non-linear dynamic analysis	1	375.17	0.0063	0.090	18.99	2.25
	2	393.44	0.0072	0.104	20.67	2.49
	3	377.09	0.0062	0.090	17.92	2.25
	4	379.69	0.0054	0.078	16.63	1.99
	5	323.37	0.0071	0.101	20.42	2.41
	6	367.41	0.0065	0.091	18.72	2.23
	7	376.91	0.0067	0.089	20.45	2.46
	8	373.19	0.0074	0.101	22.25	2.71
	9	311.63	0.0073	0.109	21.33	2.53
	10	354.11	0.0074	0.086	19.73	2.63
	Mean values	363.20	0.0068	0.094	19.71	2.39
Spectrum analysis using HFD method		335.60				

chosen for the columns beams and braces, respectively. The combination considered for dead (G) and live (Q) loads is G+0.3Q=27.5 kN/m. An elastic design spectrum for PGA=0.24 g, q=4 and soil class B is selected. Second order effects need not to be taken into account if θ<0.10. Indeed the maximum θ value found is 0.075<0.10 at the first storey of the EBF. The *IDR* for a structure having attached nonstructural elements of brittle materials, is found to satisfy $(d_r/h)\cdot v$=(0.0208/3)·0.50=0.0035<0.005 (Eurocode 8 2009).

The seismic design of the EBF under study is performed and there shall be no exceedance of the maximum link rotation angle θ_{link}=0.02 (Eurocode 8 2009). The design resulted in the following per storey column/beam/brace sections:

1st: HE280B/IPE300/CHS152.4x4,
2nd: HE280B/IPE270/CHS139.7x4,
3rd-5th: HE260B/IPE270/CHS139.7x4,
6th: HE240B/IPE270/CHS127x4,
7th: HE240B/IPE270/CHS114.3x3.6.

The EBF is then subjected to NLDA using 10 seismic motions, compatible to the aforementioned selected elastic spectrum. Response results from spectrum analysis of Eurocode 8 (2009) and from the NLDA involving maximum and mean values for base shear, IDR, top displacement (D_{top}), θ_{link} and μ_θ are provided in Table 21.

The seven-storey EBF is now designed utilizing the three considered herein methods. It should be noted that ξ_k and $\bar{q}_k$ cannot be used directly in SAP2000 (2016) since the introduction of only one value for ξ_k or $\bar{q}_k$ is permitted. Therefore, a modified design spectrum has to be constructed. In particular, this modified design spectrum is created as follows: i) for the case of ξ_k by the ordinates of the mean highly damped acceleration spectra (Fig. 3) that correspond to certain levels of modal damping and natural periods of the first four significant modes of vibration; ii) for the case of $\bar{q}_k$ by dividing the ordinates of the elastic design spectrum corresponding to the natural periods of the first four significant modes of vibration by the corresponding $\bar{q}_k$ values. The resulting modified design spectra are then inserted to SAP2000 (2016) and response spectrum analysis is performed. For both of these methods (that make use of ξ_k or $\bar{q}_k$) the resulting per storey column/beam/brace sections have as follows:

1st: HE300B/IPE300/CHS168.3x4,
2nd: HE280B/IPE300/CHS152.4x4,
3rd: HE260B/IPE270/CHS152.4x4,
4th-5th: HE260B/IPE270/CHS139.7x4,

Table 24 Results obtained by NLDA and by spectrum analysis of Eurocode 8 (2009)

	Motion	Base shear (kN)	IDR≤0.022	D_{top} (m)	μ_δ
Non-linear dynamic analysis	1	668.39	0.0097	0.131	4.13
	2	668.76	0.0114	0.110	4.93
	3	666.14	0.0081	0.088	3.50
	4	655.36	0.0084	0.084	3.63
	5	672.77	0.0101	0.095	4.35
	6	666.73	0.0120	0.102	5.30
	7	665.64	0.0098	0.092	4.17
	8	654.23	0.0076	0.108	3.35
	9	665.48	0.0109	0.101	4.71
	10	668.50	0.0099	0.102	4.20
	Mean values	665.20	0.0098	0.101	4.23
Spectrum analysis of Eurocode 8		563.82	0.0073	0.133	

Table 25 Results obtained by NLDA and by spectrum analysis using the ξ_k and $\bar{q}_k$ methods

	Motion	Base shear (kN)	IDR≤0.022	D_{top} (m)	μ_δ
Non-linear dynamic analysis	1	715.97	0.0104	0.138	4.49
	2	713.55	0.0101	0.104	4.32
	3	713.60	0.0071	0.090	3.15
	4	696.45	0.0068	0.094	3.03
	5	717.22	0.0091	0.089	3.89
	6	715.81	0.0112	0.102	4.90
	7	712.29	0.0092	0.091	3.98
	8	686.02	0.0075	0.109	3.28
	9	711.09	0.0103	0.103	4.50
	10	714.43	0.0091	0.102	3.90
	Mean values	709.64	0.0091	0.102	3.94
Spectrum analysis using ξ_k method		652.40			
Spectrum analysis using $\bar{q}_k$ method		641.50			

6th : HE240B/IPE270/CHS139.7x4,
7th: HE240B/IPE270/CHS114.3x3.6.

The designs of the two methods are expected to be the same because $\bar{q}_k$ are derived from ξ_k and hence the resulting base shears are very close to each other. The only practical difference between the methods, apart from conceptual differences, has to do with their different design spectra.

For the case of the method that utilizes ξ_k, one obtains the following values for the first four modes in terms of natural periods, damping ratios ξ_k and spectrum ordinates Sa_k: T_1=0.91 sec with $\xi_1 = 77.3\%$ and Sa_1=0.10 g; T_2=0.32 sec with $\xi_2 = 100\%$ and Sa_2 =0.18 g; T_3=0.20 sec with $\xi_3 = 100\%$ and Sa_3=0.22 g; and T_4=0.15 sec with $\xi_4 = 100\%$ and Sa_4=0.24 g. In the same way, seismic design using $\bar{q}_k$ results in the following values for the first four modes in terms of natural periods, strength reduction factors $\bar{q}_k$ and spectrum ordinates Sa_k: T_1=0.91 sec with $\bar{q}_1 = 4.14$ and Sa_1=0.10 g; T_2=0.32 sec with $\bar{q}_2 = 3.75$ and Sa_2=0.19 g; T_3=0.20 sec with $\bar{q}_3 = 3.20$ and Sa_3=0.23 g; and T_4=0.15 sec with $\bar{q}_4 = 2.85$ and Sa_4=0.25 g. Table 22 presents response results obtained by these two methods and from NLDA involving the previously mentioned 10 spectrum-compatible seismic motions. It is observed that the IDR, θ_{link} and μ_θ response values do not exceed the limit ones for the LS level, i.e., 0.022, 0.2 rad and 6.2 respectively.

Finally, the seven-storey EBF is seismically designed according to the proposed HFD method. In this case, the design procedure appears to be similar to that according to Eurocode 8 (2009), since the modified design spectrum is created simply by dividing the ordinates of the elastic design spectrum by the q_h factor. After two design iterations the resulting values are T=0.95 sec, S=7, H=21 m and by substituting them into the equations of Table 16 one obtains $\mu_{r,\max}=1.45(T^{-0.319})(S^{-0.094})(H^{0.383})=3.95$ and $q_h=1+1.96(\mu_r-1)^{0.595}=4.72$. The resulting q_h is inserted in SAP2000 (2016) and a response spectrum analysis of the EBF is performed. The resulting per storey column/beam/brace sections have as follows:

1st: HE280B/IPE300/CHS139.7x4,
2nd: HE280B/IPE270/CHS139.7x4,
3rd: HE260B/IPE270/CHS139.7x4,
4th-5th: HE260B/IPE270/CHS127x4,
6th: HE240B/IPE270/CHS127x4,
7th: HE240B/IPE270/CHS114.3x3.6.

Response results from the HFD method are compared to those of NLDA involving the 10 spectrum-compatible

Table 26 Results obtained by NLDA and by spectrum analysis using the HFD method

	Motion	Base shear (kN)	IDR≤0.022	D_{top} (m)	μ_δ
Non-linear dynamic analysis	1	635.20	0.0094	0.122	4.02
	2	638.77	0.0125	0.116	5.44
	3	634.79	0.0089	0.086	3.86
	4	610.83	0.0098	0.085	4.20
	5	640.40	0.0110	0.101	4.69
	6	635.35	0.0124	0.108	5.43
	7	635.06	0.0099	0.094	4.20
	8	625.98	0.0077	0.109	3.43
	9	635.29	0.0109	0.104	4.69
	10	636.76	0.0100	0.103	4.24
	Mean Values	632.84	0.0103	0.103	4.42
Spectrum analysis using HFD method		510.36			

Table 27 Results of the four-level seismic performance scheme employing the $\bar{q}_k$ and HFD methods and checking via NLDA

SP – EQ levels	Analysis results	Base shear (kN)		IDR ($\cdot10^{-3}$)		D_{top} (cm)		θ_{link} (rad$\cdot10^{-3}$)		μ_θ	
		$\bar{q}_k$	HFD	$\bar{q}_k$	HFD	$\bar{q}_k$	HFD	$\bar{q}_k$	HFD	$\bar{q}_k$	HFD
SP1 EQ-I	Mean	321.30	327.68	2.09	1.90	2.48	2.18	5.60	5.10	0.51	0.51
	Spectral analysis	271.40	204.32								
SP2 EQ-II	Mean	326.05	328.17	4.34	4.47	4.77	4.99	11.75	11.80	1.36	1.32
	Spectral analysis	242.20	189.80								
SP3 EQ-III	Mean	321.30	323.65	9.45	9.91	7.80	8.19	32.10	33.20	3.81	3.81
	Spectral analysis	271.40	223.04								
SP4 EQ-IV	Mean	386.56	318.82	11.14	13.31	9.90	10.15	46.50	48.16	4.69	5.72
	Spectral analysis	363.70	254.96								

seismic motions and are tabulated in Table 23.

A comparison of the results presented in Tables 21-23 reveals that i) the maximum *IDR* from the three design procedures does not exceed the limit value of 0.022 corresponding to LS level; ii) for the cases of Eurocode 8 (2009) and HFD seismic designs, mean values for θ_{link} obtained by NLDA are nearly equal; iii) for the cases of seismic designs employing either ξ_k or $\bar{q}_k$, θ_{link} is well controlled; iv) the equal displacement rule as applied in the context of Eurocode 8 (2009) leads to an overestimation of the maximum D_{top} by 15.15% and an underestimation of the maximum IDR by 7.2% against the corresponding mean D_{top} and IDR results coming from NLDA and v) in general, the two methods incorporating ξ_k and $\bar{q}_k$, appear to be more conservative than the designs with the Eurocode 8 (2009) and the HFD methods with the HFD method providing the lighter design among all methods.

7.2 BRBF for a specific IDR level

Similarly to the previous example, a steel plane BRBF of 3 bays (bay length is 5.0 m) and 7 storeys (storey height is 3.0 m) is designed with the aid of SAP2000 (2016) and properly amended provisions of Eurocode 8 (2009) for steel concentrically braced frames with chevron bracings (Bosco *et al.* 2015). Through NLDA using 10 compatible to the elastic spectrum of Eurocode 8 (2009) seismic motions, response results for the three considered herein seismic design procedures are computed. Regarding the members of the BRBF, HEB and IPE sections are selected for columns and beams, respectively, whereas a rectangular-shaped section is used to describe the steel core of the BRB (Fig. 2, right). The steel grade is S275. The combination considered for dead (*G*) and live (*Q*) loads is G+0.3Q=27.5 kN/m. An elastic design spectrum for PGA=0.36 g, q=4 and soil class B is selected. The maximum θ value found is 0.089<0.10 at the first storey of the BRBF, thus, second order effects are neglected. The *IDR* for a structure having attached nonstructural elements of brittle materials, is marginally satisfied: $(d_r/h)\cdot v$=(0.0292/3)·0.50=0.0048<0.005 (Eurocode 8 2009). The BRB frame is designed for a targeted *IDR*=0.022 utilizing the three considered herein design methods.

The resulting per storey sections for columns, beams and for the area A of the steel core of the BRB have as follows (in a column/beam/steel core format):

1st: HE340B/IPE330/A=19.5 cm^2,
2nd: HE320B/IPE330/A=17.0 cm^2,
3rd: HE300B/IPE330/A=16.2 cm^2,
4th: HE280B/IPE330/A=15.5 cm^2,
5th: HE260B/IPE330/A=15.5 cm^2,
6th: HE260B/IPE330/A=12.5 cm^2,
7th: HE240B/IPE330/A=12.5 cm^2.

Response results from spectrum analysis of Eurocode 8 (2009) and from the NLDA involving maximum and mean values for base shear, IDR, D_{top}, θ_{link} and ductility demand

μ_b of the BRB are provided in Table 24.

The seismic design according to the methods using ξ_k and $\bar{q}_k$ result in almost equal design base shears. Thus, the same member sections are found and have per storey as follows (in a column/beam/steel core format):

1st: HE360B/IPE330/A=20.6 cm^2,
2nd: HE320B/IPE330/A=19.5 cm^2,
3rd: HE300B/IPE330/A=17.0 cm^2,
4th: HE280B/IPE330/A=16.2 cm^2,
5th: HE260B/IPE330/A=15.5 cm^2,
6th: HE260B/IPE330/A=12.5 cm^2,
7th: HE240B/IPE330/A=12.5 cm^2.

For the case of the method that utilizes ξ_k, one obtains the following values for the first four modes in terms of natural periods, damping ratios ξ_k and spectrum ordinates Sa_k: T_1=0.74sec with $\xi_1 = 68.2\%$ and Sa_1=0.19 g; T_2=0.26 sec with $\xi_2 = 100\%$ and Sa_2=0.30 g; T_3=0.14 sec with $\xi_3 = 100\%$ and Sa_3=0.37 g; and T_4=0.11sec with $\xi_4 = 100\%$ and Sa_4=0.41 g. In the same way, seismic design using $\bar{q}_k$ results in the following values for the first four modes in terms of natural periods, strength reduction factors $\bar{q}_k$ and spectrum ordinates Sa_k: T_1=0.74 sec with $\bar{q}_1 = 3.75$ and Sa_1=0.19 g; T_2=0.26 sec with $\bar{q}_2 = 3.35$ and Sa_2=0.32 g; T_3=0.14 sec with $\bar{q}_3 = 2.80$ and Sa_3=0.37 g; and T_4=0.11 sec with $\bar{q}_4 = 2.10$ and Sa_4=0.43 g. Table 25 presents the response results obtained by these two methods and those coming from NLDA involving the previously mentioned 10 spectrum-compatible seismic motions.

According to the HFD method, after two design iterations the resulting values are: T=0.77 sec, S=7, H=21 m and by substituting in equations sorted in Table 17 it is shown that: $\mu_{r,\max}=6.23(T^{0.404})(S^{-0.860})(H^{0.452})=4.16$ and $q_h=1+3.24(\mu r-1)^{0.075}=4.53$. The resulting q_h is inserted in SAP2000 (2016) for the calculation of the seismic base shear and for the dimensioning of the frame members. Thus, the following member sections are found per storey (in a column/beam/steel core format):

1st: HE320B/IPE330/A=18.6 cm^2,
2nd: HE300B/IPE330/A=16.2 cm^2,
3rd: HE300B/IPE330/A=15.5 cm^2,
4th: HE280B/IPE330/A=15.5 cm^2,
5th: HE260B/IPE330/A=12.5 cm^2,
6th: HE260B/IPE330/A=12.5 cm^2,
7th: HE240B/IPE330/A=12.5 cm^2.

The response results from the HFD method are compared to those of NLDA involving the 10 spectrum-compatible seismic motions and are sorted in Table 26.

By assessing the results in Tables 24-26, the following conclusions are drawn: i) similarly to the previous example, the *IDR*=0.022 limit is not exceeded by any seismic design method; ii) the equal displacement rule as applied in the context of Eurocode 8 (2009) leads to overestimation of the maximum D_{top}, by 31.68% and underestimation of the maximum IDR by 34.2% against the corresponding mean D_{top} and IDR results coming from NLDA; iii) the design base shears resulting from Eurocode 8 (2009), HFD, ξ_k and $\bar{q}_k$ methods appear to be lower than the corresponding mean values obtained from NLDA by 17.98%, 24%, 8.77% and 10.62% respectively and iv) the HFD method and the methods using ξ_k and $\bar{q}_k$ provide quite similar mean μ_b values for the BRB, that are well below the maximum allowable values at such drift levels according to Bosco *et al.*. (2015). Finally, as in the previous example, the methods using ξ_k and $\bar{q}_k$ result in a heavier design than the other methods with the HFD method resulting in the lighter design among all other methods.

7.3 EBF for various performance levels

The three seismic design methods, are now implemented in a four-level seismic performance scheme. In particular, according to SEAOC (1999) these four performance levels and the seismic hazard associated with them have as follows: Immediate occupancy (IO/SP1) under the frequently occurred earthquake (EQ-I), Damage control (DC/SP2) under the occasional occurred earthquake (EQ-II), Life safety (LS/SP3) under the rare earthquake (EQ-III), collapse prevention (CP/SP4) under the maximum considered earthquake (EQ-IV). Table 2 provides the *IDR*, μ_θ and θ_{link} limits associated with these performance levels. The PGA corresponding to (IO/SP1), (DC/SP2), (LS/SP3) and (CP/SP4) performance levels is defined as 1/q, 0.5, 1.0 and 1.5 times the 0.24 g of the elastic response spectrum respectively, where q is the behavior factor of Eurocode 8 (2009). Employing this four-level seismic performance scheme, the maximum base shear found controls the design.

As the design incorporating ξ_k and $\bar{q}_k$ result in almost the same design base shear, only a comparison between the design by the HFD and that one by using $\bar{q}_k$ will be presented in this particular example. More specifically, a five-storey and three-bay EBF having chevron bracings and intermediate links (Fig. 1, left) is designed. Storey height, bay length, steel grade of this EBF as well as the design spectrum are the same as those considered in section 7.1. Employing the $\bar{q}_k$ and HFD methods presented herein and taking into account the four performance levels of Table 2 the following base shear (V) values and column/beam/brace sections per storey are obtained. In particular, for the case of design by using $\bar{q}_k$: i) level SP1 under EQ-I: T_1=0.83 sec and $\bar{q}_1$=1.00, T_2=0.28 sec and $\bar{q}_2$=1.00, T_3=0.16sec and $\bar{q}_3$=1.00, T_4=0.11 sec and $\bar{q}_4$=1.00, V=271.40 kN and hence the per story sections read as follows:

1st: HE300B/IPE240/CHS152.4x4,
2nd: HE280B/IPE240/CHS139.7x4,
3rd: HE260B/IPE240/CHS127x4,
4th-5th: HE240B/IPE240/CHS114.3x3.6.

ii) level SP2 under EQ-II: T_1=0.84 sec and $\bar{q}_1$=2.11, T_2=0.29 sec and $\bar{q}_2$=1.48, T_3=0.16 sec and $\bar{q}_3$=3.00, T_4=0.11 sec and $\bar{q}_4$ = 2.20, V=242.20 kN and hence the per storey sections read as follows:

1st: HE300B/IPE240/CHS139.7x4,
2nd: HE280B/IPE240/CHS139.7x4,
3rd: HE260B/IPE240/CHS127x4,
4th: HE260B/IPE240/CHS114.3x3.6,
5th: HE260B/IPE240/CHS114.3x3.6.

iii) level SP3 under EQ-III: T_1=0.83 sec and $\bar{q}_1$=3.56, T_2=0.28 sec and $\bar{q}_2$=3.47, T_3=0.16 sec and $\bar{q}_3$=3.00, T_4=0.11 sec and $\bar{q}_4$=2.20, V=271.40 kN and hence the per storey sections read as follows:

1st: HE300B/IPE240/CHS152.4x4,
2nd: HE280B/IPE240/CHS139.7x4,
3rd: HE280B/IPE240/CHS127x4,

4th-5th: HE240B/IPE240/CHS114.3x3.6.

iv) level SP4 under EQ-IV: T_1=0.82 sec and $\bar{q}_1$=4.02, T_2=0.27 sec and $\bar{q}_2$=3.43, T_3=0.16 sec and $\bar{q}_3$=3.00, T_4=0.11 sec and $\bar{q}_4$=2.20, V=363.70 kN and hence the per storey sections read as follows:

1st : HE300B/IPE270/CHS168.3x4,
2nd: HE280B/IPE240/CHS152.4x4,
3rd : HE260B/IPE240/CHS139.7x4,
4th: HE260B/IPE240/CHS127x4,
5th: HE260B/IPE240/CHS114.3 x3.6.

Similarly, for the case of design using the HFD: i) level SP1 under EQ-I: T=0.87 sec and q_h=1.12; V=204.32 kN and hence the per storey sections read as follows:

1st: HE300B/IPE240/CHS127.4x4,
2nd: HE280B/IPE240/CHS127.4x4,
3rd: HE260B/IPE240/CHS114.3x3.6,
4th: HE260B/IPE240/CHS114.3x3.6,
5th: HE260B/IPE240/CHS108x3.6.

ii) level SP2 under EQ-II: T=0.87 sec and q_h=2.82; V=189.80 KN and hence the per storey sections read as follows:

1st: HE300B/IPE240/CHS127.4x4,
2nd: HE280B/IPE240/CHS127.4x4,
3rd: HE280B/IPE240/CHS114.3x3.6,
4th-5th: HE260B/IPE240/CHS108x3.6.

iii) level SP3 under EQ-III: T=0.86 sec and q_h=4.55; V=223.04 kN and hence the per storey sections read as follows:

1st: HE300B/IPE240/CHS139.7x4,
2nd: HE280B/IPE240/CHS127x4,
3rd: HE260B/IPE240/CHS114.3x3.6,
4th: HE260B/IPE240/CHS114.3x3.6,
5th: HE260B/IPE240/CHS108x3.6.

iv) level SP4 under EQ-IV: T=0.84 sec and q_h=5.93; V=254.96 kN and hence the per storey sections read as follows:

1st: HE300B/IPE240/CHS159x4,
2nd: HE280B/IPE240/CHS139.7x4,
3rd: HE280B/IPE240/CHS127x4,
4th: HE260B/IPE240/CHS114.3x3.6,
5th: HE260B/IPE240/CHS108x3.6.

Response results of this four-level seismic performance scheme are compared to those coming from NLDA of the designed frames under 10 seismic motions, compatible to the elastic spectra defined for 1/q, 0.5, 1.0 and 1.5 times 0.24 g. These response results involve maximum and mean values for base shear, IDR, D_{top}, θ_{link} and μ_θ and are shown in Table 27.

By observing the results of Table 27, one concludes that for both the $\bar{q}_k$ and HFD methods, the level SP4 under EQ-IV leads to the maximum base shear, i.e., 363.70 kN and 254.96 KN for the $\bar{q}_k$ and HFD methods, respectively, and essentially controls the design. Furthermore, the IDR, μ_θ and θ_{link} limits of Table 2 are not exceeded by the results of NLDA presented in Table 27. Finally, once again, the seismic design through $\bar{q}_k$ is proved to be more conservative in comparison to that using the HFD method.

The results of the two compared methods, which are shown in Table 27 and account for the pair SP3 - EQ-III, are comparable to those of Eurocode 8 (2009) that by default correspond to the LS performance level. To this end, the same frame is designed according to Eurocode 8 (2009), using q=4 which is applicable to the medium ductility class (DCM) case. The maximum θ value found is 0.055<0.10, thus, second order effects are neglected. Furthermore, there is no limitation of the IDR occurring by the frequent earthquake because $(d_r/h)\cdot v$=(0.0264/3)·0.5=0.0044<0.005. Spectrum analysis for T=0.85 sec leads to base shear V=249 kN and provides the following per storey column/beam/brace sections:

Table 28 Results obtained by NLDA and by spectrum analysis of Eurocode 8 (2009)

	Base shear (kN)	IDR (10^{-3})	D_{top} (cm)	θ_{link} (rad·10^{-3})	μ_θ
Mean values	323.43	9.76	8.06	32.90	3.78
Spectral analysis	249.00	8.80	10.0		

1st: HE300B/IPE240/CHS139.7x4,
2nd: HE280B/IPE240/CHS127x4,
3rd: HE260B/IPE240/CHS127x4,
4th: HE260B/IPE240/CHS114.3x3.6,
5th: HE260B/IPE240/CHS108x3.6.

The mean values of the results of NLDA with those of the corresponding spectrum analysis of Eurocode 8 (2009) are summarized in Table 28. According to Table 28, the seismic design using Eurocode 8 (2009) does not exceed the IDR, μ_θ and θ_{link} limit values presented in Table 2. Furthermore, it appears once again that the seismic design with the use of the HFD method is the most economical.

8. Conclusions

Given the preceding developments, the following conclusions can be stated:

1. Three performance-based seismic design methods of the force-based type, the ones incorporating ξ_k and $\bar{q}_k$, developed by the authors elsewhere and the HFD method incorporating a behavior factor q_h, developed by the authors herein, for the seismic design of plane steel EBFs and BRBFs have been compared. Explicit expressions for the calculation of all three factors ξ_k, $\bar{q}_k$ and q_h have been provided for the four soil classes (A-D) of Eurocode 8 (2009) and various seismic performance levels. The comparison among the three methods and against the Eurocode 8 (2009) design method has been done with the aid of nonlinear dynamic analyses via representative numerical examples.
2. The three proposed seismic design methods constitute a trustworthy solution for the cases of steel EBFs and BRBFs, since the corresponding non-linear analyses proved that the designed frames develop a desirable seismic behavior, without exceeding the upper deformation/damage limits stipulated by seismic codes (SEAOC 1999). All three methods, when used only for the LS performance level, produce the design in only one step (checking only strength) and not in two steps (checking both strength and displacement) as it is the case with the Eurocode 8 (2009) method. This is because in these three methods the ξ_k, $\bar{q}_k$ and q_h

factors are deformation-dependent and hence displacement requirements are automatically satisfied.

3. The seismic design methods using ξ_k or $\bar{q}_k$ provide very close values for base shears and hence the same designs, which are more conservative than those of the Eurocode 8 (2009) and HFD methods. They are also more accurate because of their higher degree of rationality. However, they produce only base shears and not deformations, since the equal displacement rule is not applicable here as it is the case with the Eurocode 8 (2009) and HFD methods, which have a single behavior factor. Nevertheless, as it was pointed out in conclusion No 2, no deformation checking is needed in all three considered methods. Furthermore, use of the first two considered methods is more difficult because they require the insertion of a modified spectrum in the seismic design software.

4. All three methods are true performance-based seismic design methods that can accommodate more than two performance levels. It was also shown that the HFD method leads to the most economical design even compared to Eurocode 8 (2009). Furthermore, by observing the results of the seismic design with Eurocode 8 (2009) method, it appears that the frame damage is underestimated since the equal displacement rule results in lower values of *IDR* in relation to the NLTH analysis and this may lead to unsafe design.

5. Out of the three considered seismic design methods, it appears that the HFD method is a better choice because of its simplicity, acceptable accuracy and better deformation control. The method is also capable of estimating displacements by using the equal displacement rule because it employs a single behavior factor, but since checking of displacements is automatically satisfied, there is no reason to exercise this capability, especially when the results are approximate and not very reliable.

References

ASCE/SEI 7-16 (2017), Minimum Design Loads and Associated Criteria for Buildings and other Structures, American Society of Civil Engineers; Reston, Virginia, U.S.A.

Bosco, M., Marino, E.M. and Rossi, P.P. (2015), “Design of steel frames equipped with BRBs in the framework of Eurocode 8”, *J. Constr. Steel Res.*, **113**, 43-57. https://doi.org/10.1016/j.jcsr.2015.05.016.

Caprili, S., Mussini, N. and Salvatore, W. (2018), “Experimental and numerical assessment of EBF structures with shear links”, *Steel Compos. Struct.*, **28**(2), 123-138. http://doi.org/10.12989/scs.2018.28.2.123.

Carr, A.J. (2007), RUAUMOKO 2D: User Manual for the 2-Dimensional Version, University of Canterbury, Canterbury, New Zealand.

Eskandari, R. and Vafaei, D. (2015), “Effects of near-fault records characteristics on seismic performance of eccentrically braced frames”, *Struct. Eng. Mech.*, **56**(5), 855-870. http://doi.org/10.12989/sem.2015.56.5.855

Eurocode 3 (2005), Design of Steel Structures. Part 1.1: General Rules and Rules for Buildings, European Committee for Standardization, Brussels, Belgium.

Eurocode 8 (2009), Design of Structures for Earthquake Resistance. Part 1.1: General Rules, Seismic Actions and Rules for Buildings, European Committee for Standardization, Brussels, Belgium.

Gleize, J. and Koboevic, S. (2014), “Study of global seismic response of eccentrically braced frames with long links”, *Proceedings of the 9th International Conference on Structural Dynamics (EYRODYN)*, Porto, Portugal, June.

Hatzigeorgiou, G.D. (2010), “Damping modification factors for SDOF systems subjected to near-fault, far-fault and artificial earthquakes”, *Earthq. Eng. Struct. Dyn.*, **39**(11), 1239-1258. https://doi.org/10.1002/eqe.991.

Hsiao, P.C., Lehman, D.E. and Roeder, C.W. (2012), “Improved analytical model for special concentrically braced frames”, *J. Constr. Steel Res.*, **73**, 80-94. https://doi.org/10.1016/j.jcsr.2012.01.010.

Kalapodis, N.A. (2017), “Seismic design of steel plane braced frames with the use of three new methods”, Ph.D. Dissertation, University of Patras, Patras, Greece.

Kalapodis, N.A. and Papagiannopoulos, G.A. (2020), “Seismic design of plane steel braced frames using equivalent modal damping ratios”, *Soil Dyn. Earthq. Eng.*, **129**, 105947. https://doi.org/10.1016/j.soildyn.2019.105947.

Kalapodis, N.A., Papagiannopoulos, G.A. and Beskos, D.E. (2018), “Modal strength reduction factors for seismic design of plane steel braced frames”, *J. Constr. Steel Res.*, **147**, 549-563. https://doi.org/10.1016/j.jcsr.2018.05.004.

Karavasilis, T.L., Bazeos, N. and Beskos, D.E. (2006), “A hybrid force/displacement seismic design method for plane steel frames”, *Proceedings of the 5th International Conference on Behavior of Steel Structures in Seismic Areas (STESSA)*, Yokohama, Japan, October.

Kazemzadeh Azad, S. and Topkaya, C. (2017), “A review of research on steel eccentrically braced frames”, *J. Constr. Steel Res.*, **128**, 53-73. https://doi.org/10.1016/j.jcsr.2016.07.032.

Lee, C.H., Jeon, S.W., Kim, J.H. and Uang, C.M. (2005), “Effects of panel zone strength and beam web connection method on seismic performance of reduced beam section steel moment connections”, *J. Struct. Eng.*, **131**(12), 1854-1865. https://doi.org/10.1061/(ASCE)0733-9445(2005)131:12(1854).

Li, S., Tian, J.B. and Liu, Y.H. (2017), “Performance-based seismic design of eccentrically braced steel frames using target drift and failure mode”, *Earthq. Struct.*, **13**(5), 443-454. http://doi.org/10.12989/eas.2017.13.5.443.

Loulelis, D.G., Papagiannopoulos, G.A. and Beskos, D.E. (2018), “Modal strength reduction factors for seismic design of steel moment resisting frames”, *Eng. Struct.*, **154**(1), 23-37. https://doi.org/10.1016/j.engstruct.2017.10.071.

MATLAB (2015), Matlab Documentation; MathWorks Inc., Massachusetts, U.S.A. https://www.mathworks.com.

Muho, E.V., Papagiannopoulos, G.A. and Beskos, D.E. (2019a), “A seismic design method for reinforced concrete moment resisting frames using modal strength reduction factors”, *Bull. Earthq. Eng.*, **17**(1), 337-390. https://doi.org/10.1007/s10518-018-0436-3.

Muho, E.V., Papagiannopoulos, G.A. and Beskos, D.E. (2019b), “Deformation dependent equivalent modal damping ratios for the performance-based seismic design of plane R/C structures”, *Soil Dyn. Earthq. Eng.*, **129**. https://doi.org/10.1016/j.soildyn.2018.08.026

Okazaki, T., Lignos, D.G., Hikino, T. and Kajiwara, K. (2013), “Dynamic response of a chevron concentrically braced frame”, *J. Struct. Eng.*, **139**(4), 515-525. https://doi.org/10.1061/(ASCE)ST.1943-541X.0000679.

Papagiannopoulos, G.A. (2018), “Jacobsen’s equivalent damping concept revisited”, *Soil Dyn. Earthq. Eng.*, **115**, 82-89. https://doi.org/10.1016/j.soildyn.2018.08.001.

Papagiannopoulos, G.A. and Beskos, D.E. (2010), “Towards a seismic design method for plane steel frames using equivalent modal damping ratios", *Soil Dyn. Earthq. Eng.*, **30**(10), 1106-1118. https://doi.org/10.1016/j.soildyn.2010.04.021.

Papagiannopoulos, G.A. and Beskos, D.E. (2011), "Modal strength reduction factors for seismic design of plane steel frames", *Earthq. Struct.*, **2**(1), 65-88. http://doi.org/10.12989/eas.2011.2.1.065.

PEER (2013), https://ngawest2.berkeley.edu.

Pian, C., Qian, J., Muho, E.V. and Beskos, D.E. (2019), "A hybrid force/displacement seismic design method for reinforced concrete moment resisting frames", *Soil Dyn. Earthq. Eng.*, **129**. https://doi.org/10.1016/j.soildyn.2018.09.002.

Priestley, M.J.N., Calvi, G.M. and Kowalsky, M.J. (2007), *Displacement-Based Seismic Design of Structures*, IUSS Press, Pavia, Italy.

Qi, Y., Li, W. and Feng, W. (2017), "Seismic collapse probability of eccentrically braced steel frames", *Steel Compos. Struct.*, **24**(1), 37-52. http://doi.org/10.12989/scs.2017.24.1.037.

Salawdeh, S. and Goggins, J. (2011), "Direct displacement based seismic design for single storey steel concentrically braced frames", *Earthq. Struct.*, **10**(5), 1125-1141. http://dx.doi.org/10.12989/eas.2016.10.5.1125.

SAP2000 (2016), Analysis Reference Manual, Computers and Structures Inc., Berkeley. https://www.csiamerica.com/

SEAOC (1999), Recommended Lateral force Requirements and Commentary, Structural Engineers Association of California; Sacramento, California, U.S.A.

Skalomenos, K.A., Hatzigeorgiou, G.D. and Beskos, D.E. (2015), "Application of the hybrid force/displacement (HFD) seismic design method to composite steel/concrete plane frames", *J. Constr. Steel Res.*, **115**, 179-190. https://doi.org/10.1016/j.jcsr.2015.08.007.

Tzimas, A.S., Karavasilis, T.L., Bazeos, N. and Beskos, D.E. (2013), "A hybrid force/displacement seismic design method for steel building frames", *Eng. Struct.*, **56**, 1452-1463. https://doi.org/10.1016/j.engstruct.2013.07.014.

CC